

# The ProtoDUNE-SP LArTPC Electronics Production, Commissioning, and Performance

**D. Adams<sup>b</sup> M. Bass<sup>b</sup> M. Bishai<sup>b</sup> C. Bromberg<sup>m</sup> J. Calcutt<sup>m</sup> H. Chen<sup>b</sup> J. Fried<sup>b</sup>  
I. Furic<sup>f</sup> S. Gao<sup>b</sup> D. Gastler<sup>a</sup> J. Hugon<sup>l</sup> J. Joshi<sup>b</sup> B. Kirby<sup>b</sup> F. Liu<sup>s</sup> K. Mahn<sup>m</sup>  
M. Mooney<sup>d</sup> C. Morris<sup>h</sup> C. Pereyra<sup>c</sup> X. Pons<sup>e</sup> V. Radeka<sup>b</sup> E. Raguzin<sup>b</sup> D. Shooltz<sup>m</sup>  
M. Spanu<sup>b</sup> A. Timilsina<sup>b</sup> S. Tufanli<sup>v(1)</sup> M. Tzanov<sup>l</sup> B. Viren<sup>b</sup> W. Gu<sup>b</sup> Z. Williams<sup>p</sup>  
K. Wood<sup>n</sup> E. Worcester<sup>b</sup> M. Worcester<sup>b</sup> G. Yang<sup>n</sup> J. Zhang<sup>b</sup>**

<sup>a</sup>*Boston University, Boston, MA, 02215, USA*

<sup>b</sup>*Brookhaven National Laboratory (BNL), Upton, NY, 11973, USA*

<sup>c</sup>*University of California (Davis), Davis, CA 95616, USA*

<sup>d</sup>*Colorado State University, Fort Collins, CO 80523, USA*

<sup>e</sup>*European Organization for Nuclear Research (CERN), Geneva, 1211, Switzerland*

<sup>f</sup>*University of Florida, Gainesville, FL 32611, USA*

<sup>h</sup>*University of Houston, Houston, TX 77204, USA*

<sup>l</sup>*Louisiana State University, Baton Rouge, LA 70803, USA*

<sup>m</sup>*Michigan State University, East Lansing, MI 48824, USA*

<sup>n</sup>*Stony Brook University, Stony Brook, New York 11794, USA*

<sup>p</sup>*University of Texas (Arlington), Arlington, TX 76019, USA*

<sup>s</sup>*Tsinghua University, Beijing, 10084, China*

<sup>v</sup>*Yale University, New Haven, CT 06520, USA*

*E-mail: [mspanu@bnl.gov](mailto:mspanu@bnl.gov)*

**ABSTRACT:** The ProtoDUNE-SP detector is a large-scale prototype of the Single-Phase (SP) Liquid Argon Time Projection Chamber (LArTPC) design proposed for the Deep Underground Neutrino Experiment (DUNE). 15,360 LArTPC wires are instrumented with low electronic noise pre-amplifier and digitization ASICs integrated into Front End Motherboards (FEMBs) operating at cryogenic temperature within the cryostat. The large number of electronics channels and high performance specifications required a large-scale production electronics quality control effort, careful installation into Anode Plane Assemblies (APAs), and rigorous detector commissioning. This successful collaboration-wide effort achieved a working LArTPC electronics channel percentage of 99.7% (15,318 of 15,360 channels in total), with operating at electronic levels above expectation. We summarize the ProtoDUNE-SP cold electronics design and quality control, installation, and commissioning efforts that enabled this excellent electronics performance. <sup>1</sup>

**KEYWORDS:** ProtoDUNE, Electronics

<sup>1</sup>Now at European Organization for Nuclear Research (CERN), Geneva, 1211, Switzerland

---

## Contents

<b>1</b>	<b>Introduction</b>	<b>2</b>
1.1	TPC Readout System Design	3
1.1.1	Cold Electronics	4
1.1.2	Warm Interface Electronics	7
<b>2</b>	<b>Production Electronics Quality Control</b>	<b>8</b>
2.1	Test Stand Software and Data Management	9
2.2	Oscillator Tests	9
2.3	Flash Memory Tests	10
2.4	FE ASIC Tests	11
2.4.1	Warm Screening	11
2.4.2	Cold Screening	12
2.5	ADC ASIC Tests and Selection	13
2.6	Warm Interface Electronics Tests	16
2.7	FEMB and CE Box Tests	17
2.8	Cryogenic Test System	19
2.9	Summary and Lessons for Future LArTPC Experiments	20
<b>3</b>	<b>Installation</b>	<b>21</b>
3.1	Reception test and installation	21
3.2	Cold Box Integration Test	23
<b>4</b>	<b>Commissioning</b>	<b>25</b>
4.1	Electronics Performance	26
4.2	Clock failure on FEMB302	28
<b>5</b>	<b>Conclusion</b>	<b>30</b>

---

## 1 Introduction

The Deep Underground Neutrino Experiment (DUNE) is a next-generation neutrino oscillation experiment. DUNE's scientific goals include precise measurements of the parameters governing long-baseline neutrino oscillation, including sensitivity to CP-violation discovery, as well as sensitivity to neutrinos from core-collapse supernovae and a variety of BSM physics including baryon number violating processes. DUNE will consist of an intense long-baseline neutrino beam from Fermi National Accelerator Laboratory in Batavia, Illinois, to the Sanford Underground Research Laboratory in South Dakota, approximately 1300 kilometers downstream of the source [1]. A Near Detector (ND) installed at Fermilab will record particle interactions near the beam source, whereas a massive Far Detector (FD) consisting of four Liquid Argon Time Projection Chambers (LArTPC) holding in total around 68 ktons LAr, will be constructed at the Sanford Lab site. The collaboration has undertaken an extensive prototype program (protoDUNE) at CERN Neutrino Platform facility to establish the design and performance of two variants of the LArTPC technology: Single-Phase [2] and Dual-Phase [3].

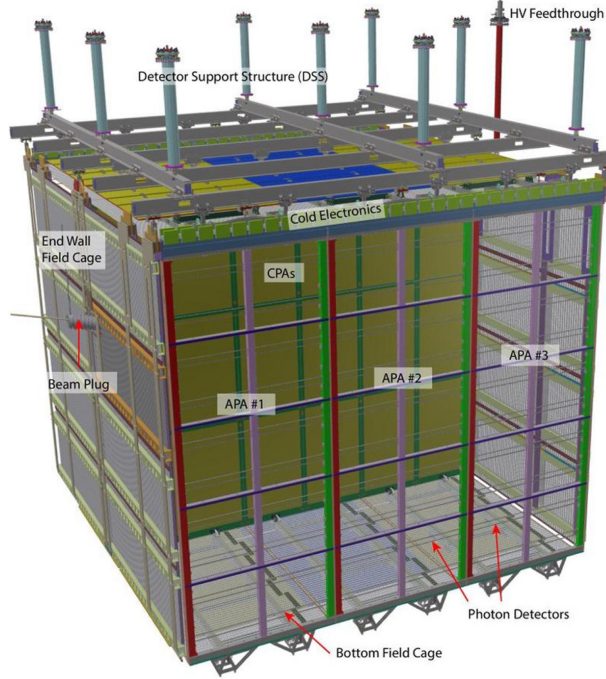


**Figure 1:** protoDUNE Single-Phase LArTPC schematic design. The TPC readout Cold Electronics are indicated by the green boxes along the top of each APA.

The aim of the protoDUNE program is to better define the production and installation procedures for the DUNE FD as well as accumulate test-beam data at CERN in order to measure the response of the detector to different particles at energies in the 0.5 – 7 GeV range. Containing 770 tons of LAr (411 tons active volume) protoDUNE Single-Phase (SP) consists of six full-size Anode Plane Assemblies (APAs) for a total of 15,360 TPC sense wire and electronics channels [4]. The 500 V/cm electric field is produced by three Cathode Plane Assemblies (CPA) installed in the inner part of the TPC for a total of  $2 \times 3.6$  meter drift regions, each observed by three APAs, as shown

in Figure 1. Sixteen field cage aluminium profiles maintain a uniform electric field between the cathode and anode. The top and bottom of the TPC are equipped with perforated stainless steel ground planes to ensure no field outside the active volume. The detector is located in an extension to the EHN1 hall at CERN and it took its first beam-data from the new H4-VLE beam line before the LHC long shutdown at the end of 2018. The H4-VLE beam line comes from an extension of the secondary +80 GeV/c pions beam line, which comes in turn from a first extension of the 400 GeV/c primary beam from SPS. It consists of tertiary  $e^-$ ,  $p$ ,  $\mu^+$ ,  $\pi^+$  beam with energy range from a 0.5 to 7 GeV/c.

Electronics noise is characterized by equivalent noise charge (ENC) which is defined as the number of instantaneous electrons collected at the input of the readout amplification required to produce a signal of magnitude equal to a measured noise RMS.

For the entire drift region to be fully active the ENC is required to be less than  $\sim 1/9$  that of a signal arising from a minimum ionizing particle. This corresponds to an  $ENC < 1000 e^-$  in the case that LAr has a purity such that drifting electrons have a mean lifetime of 3 msec.

To achieve this, a TPC readout "Cold Electronics" design integrated with the detector electrodes has been developed for cryogenic temperatures (77 – 89 K). In this configuration the length of signal carrying wires may be minimized and thermal noise is reduced, so that the ENC is independent of the fiducial volume and lower than with readout electronics at room temperature [5].

## 1.1 TPC Readout System Design

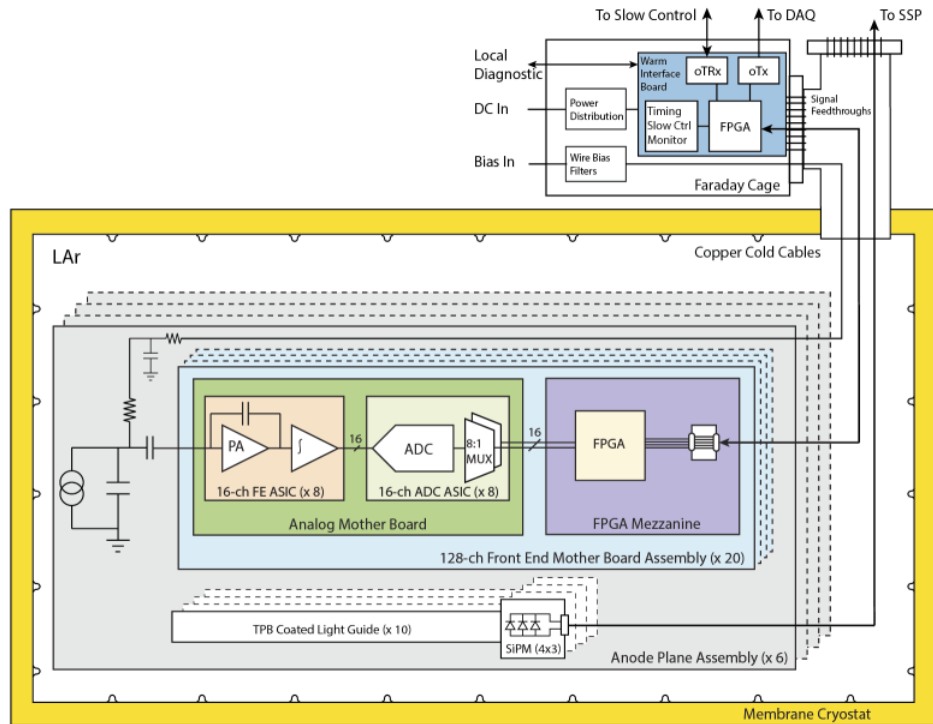


**Figure 2:** The protoDUNE-SP CE architecture. All components inside the Membrane Cryostat are operating submerged in LAr at 89K.

Element	Quantity	Channels per element
Front-End Mother Board (FEMB)	120, 20 per APA	128
FE ASIC	960, 8 per FEMB	16
ADC ASIC	960, 8 per FEMB	16
FPGA	120, 1 per FEMB	128
Cold cables	120, 1 per FEMB	128
CE feedthrough	6, 1 per APA	2560
Signal flange	6, 1 per APA	2560
Warm Interface Electronics Crate (WIEC)	6, 1 per APA	2560
Warm Interface Board (WIB)	30, 5 per WIEC	512
Power and Timing Card (PTC)	6, 1 per WIEC	2560
Power and Timing Backplane (PTB)	6, 1 per WIEC	2560

**Table 1:** Components of the CE system.

The ProtoDUNE-SP Cold Electronics (CE) system is shown in Figure 2 [6] [7]. The CE provides deadtimeless signal handling and transmission from the detector electrodes directly on the Anode Plane Assembly (APA), sketched to the left of the Analog Mother Board input, until the data is received by the ProtoDUNE-SP Data Acquisition (DAQ) and Slow Control computers over optical fibers, represented in figure by the arrows from the Warm Interface Board outside of the cryostat.

### 1.1.1 Cold Electronics

The cryogenic elements of the CE system consist of 20 Front-End Mother Boards (FEMBs) installed close to the wire electrodes on top of each APA, which are composed of three wire planes (2 induction and one collection plane) for a total of 15,360 wires. The FEMB amplify, shape, digitize, and transmit all the TPC channels to the warm interface electronics through cold data cables. Each FEMB contains one Analog Motherboard, which is assembled with eight 16-channel analog Front-End (FE) ASICs [8], which provide amplification and pulse shaping, and eight 16-channel Analog to Digital Converter (ADC) ASICs for a total of 128 channel readout per FEMB, as listed in Table 1. Both the FE and ADC ASICs are custom circuits designed at Brookhaven National Laboratory (BNL) implemented with the TSMC 180 nm CMOS process and operate at 1.8 Volts, with very low power consumption to increase the ASIC lifetime in cold, in order to operate the DUNE FD without significant loss of channels for the 20+ years required by the physics program [1].

Because the FE ASIC amplifier inputs are attached directly to the APA, ENC from additional capacitance is minimized. Additionally, due to the CMOS static characteristic at cryogenic temperature [9], the ENC of these ASICs decreases at cryogenic temperature, enabling very low ENC operation. Finally, because the signals are digitized before transmission outside the cryostat, the cryostat penetrations for signal feed-through (a possible source of excess noise) are simplified and the design of the CE system is uncoupled from elements of the TPC design, *e.g.* cable length from APA to signal feed-through.

The FE ASIC is three design revisions from the version of the ASIC deployed in the MicroBooNE detector [10]. Each FE ASIC channel has a dual-stage charge amplifier circuit with a programmable gain selectable from 4.7, 7.8, 14 and 25 mV/fC (full scale charge of 55, 100, 180 and 300 fC), a

5th-order anti-aliasing shaper with programmable time constant (peaking time 0.5, 1, 2, and 3  $\mu$ s), an option to enable AC coupling, and a baseline adjustment for operation at either 200 mV for the unipolar pulses on the collection wires or 900 mV for the bipolar pulses on the induction wires, as shown in Figure 3. Each FE ASIC also has an adjustable pre-amplifier leakage current selectable from 100, 500, 1000, and 5000 pA. The estimated power dissipation of a FE ASIC is about 5.5 mW per channel at 1.8 V.

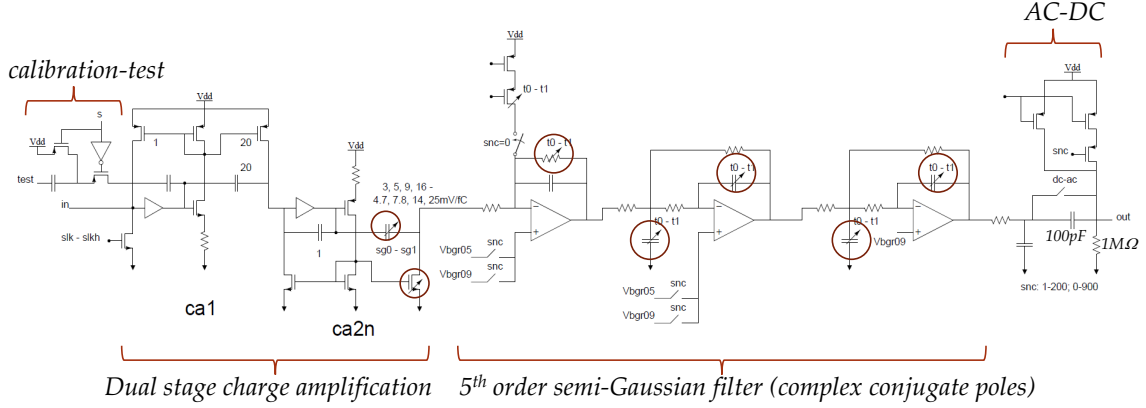


**Figure 3:** Channel schematic of the FE ASIC, which includes a dual-stage charge amplifier and a 5th-order shaper with complex conjugate poles. Circuits in red circles are programmable to allow different gain and peaking time settings.

Each FE ASIC contains a programmable pulse generator with a 6-bit DAC for electronics calibration, which is connected to each channel individually via an injection capacitor labelled *calibration-test* in Figure 3. The injection capacitor is 184 fF at room temperature and 183 fF at 77K, with measured channel-to-channel variation typically less than 1%. At cryogenic temperature the packaging of the FE ASIC puts excessive pressure on the ASIC chip. The version of the FE ASIC used in ProtoDUNE-SP responds to this stress with a channel dependent non-uniform lowering, called "drop-out", by up to 150 mV of its collection mode baseline of 200mV. This results in some channels on few ASICs operating below the minimum acceptable voltage in LAr, which compromised the channel performance. In addition, when the baseline is that low, the amplifier is no longer in its linear range. This issue was not observable at room temperature.

The ADC ASIC has 16 independent 12-bit digitizers performing at speeds up to 2 megasamples per second (MS/s), local buffering, and an 8:1 multiplexing stage with two pairs of serial readout lines in parallel. Each ADC samples the input voltage in the range 0.2 – 1.6 V and passes the digitized sample to a built-in FIFO block, 32 bits deep and 192 (16×12) bits wide, and has full and empty indicator flags, needed for interfacing to the FPGA. The estimated power dissipation of an ADC ASIC is less than 5 mW per channel at 1.8 V.

The version of the ADC ASIC used in ProtoDUNE-SP suffered from several issues at cryogenic temperature, which were non-observable at room temperature. The most significant issue with this ASIC was "sticky codes," in which certain ADC values would be preferentially populated by the ADC independent of the input voltage, causing the readout channel to appear to "stick" at a particular value, as shown in Figure 4. The "domino" architecture [11] used in this design relies



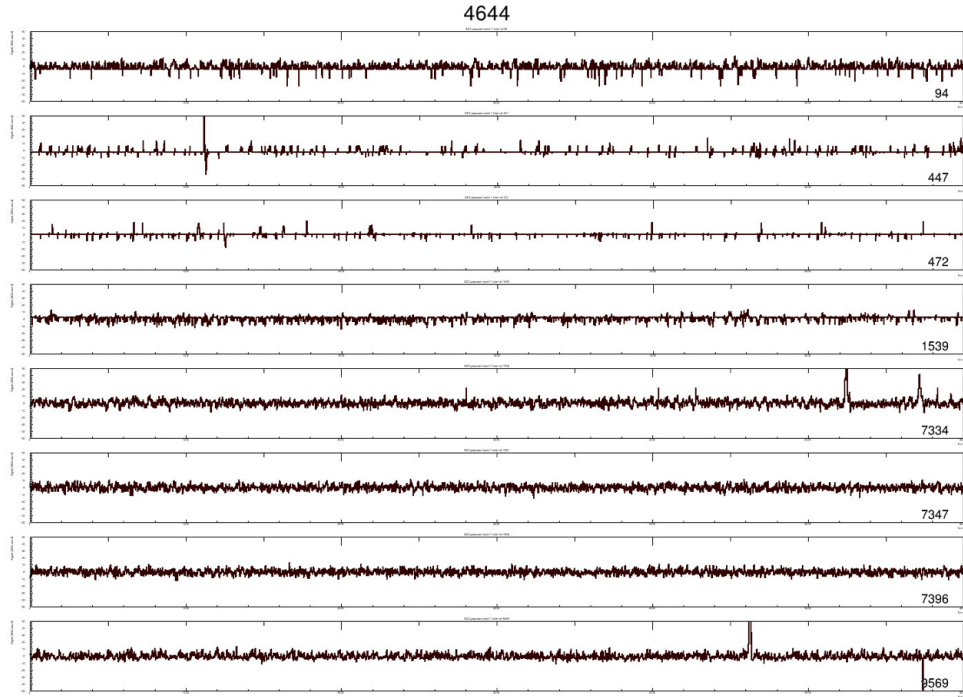


**Figure 4:** Representative waveforms from ProtoDUNE-SP run 4644, with the y-axis from -50 to 50 ADC counts and the x-axis in time-ordered 500 ns ticks. The top four show sticky code behavior from the ADC near the channel baseline, with channels 447 and 472 severely impacted. For comparison, the bottom four channels do not exhibit sticky code effects, showing the normal level of RMS fluctuation near the baseline.

on excellent transistor matching, which is difficult to simulate at LAr temperature. The flaw in this ADC design was identified as a failure of transistor matching at the transition from digitizing the 6 most significant bits to the 6 least significant bits: therefore, the sticky codes tended to prefer multiples of 0 and 63 in the ADC dynamic range.

A commercial Altera Cyclone IV FPGA, assembled on a mezzanine card which was attached to the Analog Motherboard, provided clock and control signals to the FE and ADC ASICs. The Cyclone IV was not designed for operation at cryogenic temperature; its performance in 77 – 89K was validated by standalone tests in LN2. The FPGA also further serialized the 16 data streams from the ADCs into four 1.25 Gbps links for transmission to the warm interface electronics (Section 1.1.2). The FPGA could also provide a calibration pulse to each FE ASIC channel via the same injection capacitor as used for the internal FE ASIC DAC, as a cross-check for the electronics calibration. In order to program the FPGA upon start-up, the FPGA mezzanine card contains a commercial Altera EPCS64SI16N 64 Mbit flash memory chip, which was also not designed for cryogenic operation and required standalone validation tests in LN2.

Two sets of 7-meter long cold cable bundles provide power, clock, control, and data signals between the CE flange and the FEMBs. The cold data cables for each FEMB contain 12 twin-axial 26 AWG separately-shielded cables carrying the following differential signals (shown in Figure 6): four

1.25 Gbps data links from the FEMB to the WIB, four JTAG programming signals as a backup to program the FEMB FPGA, and two system clocks at 100 MHz and 2 MHz and two I<sup>2</sup>C-like control links from the WIB to the FEMBs. The LV power cables contained 9 twisted-pair 20 AWG wires, carrying 1.5V, 2.5V, 3.0V, 4.2V and 5V. These voltages were further stepped down by linear power regulators onboard the FEMB. Shorting caps for both types of cable were designed to make a low-impedance connection between the signal lines and ground return lines to prevent charge accumulation on the cables during handling, which could cause electrostatic discharge (ESD) damage to the FEMBs.

### 1.1.2 Warm Interface Electronics

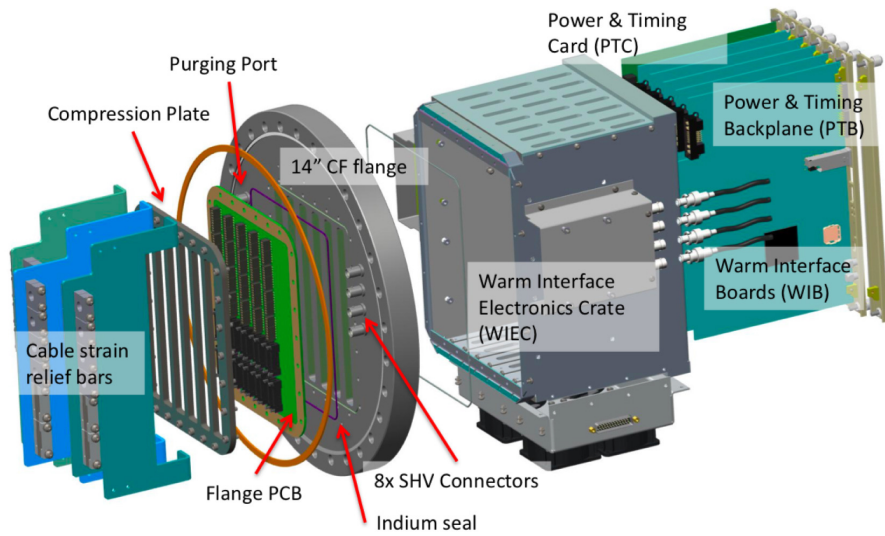


**Figure 5:** Schematic design of the WIEC and components of the warm interface electronics.

The warm interface electronics is the interface between the CE and DAQ/timing systems. It is housed in the Warm Interface Electronics Crates (WIECs) attached directly to the signal flanges. Each WIEC has one Power and Timing Card (PTC), five Warm Interface Boards (WIBs) and a passive Power and Timing Backplane (PTB), as shown in Figure 5. A flange PCB board with only surface mount components to prevent air leakage into the cryostat carries all CE signals in and out of the cryostat.

The PTC provides both a bidirectional fiber optical link to the timing system and the input of the 48 V power to the WIEC. It steps down the 48 V to up to six 12 V lines and fans out 12 V power and clock signals to WIBs over the PTB. The WIB provides both local power and control for up to 4 FEMBs, and includes a real-time digital diagnostic readout on a dedicated gigabit Ethernet (GbE) UDP link. Each WIB is controlled by an Altera Arria V GT FPGA and is powered by 12 V. DC/DC converters onboard the WIB further step down the 12 V to 9 power lines between 1.5 and 5 V for each FEMB and transmit the power over the cold LV power cables, as shown in Figure 6.

The WIB receives and decodes the timing system clock and commands with an Analog Devices ADN2184 clock/data separator. It further processes the clock with a Silicon Labs Si5344 jitter cleaner before it forwards the system clock and timing signals to the FEMBs, including the 100 MHz





fully assembled FEMBs at room and cryogenic temperature to speed up production and improve reliability.

## **2.1 Test Stand Software and Data Management**

A Python-based software framework was implemented to automate component testing and evaluation for production QC [12]. Individual test stands used a Python script to coordinate the entire testing process for a specific type of component. These scripts controlled and configured test hardware, recorded relevant data and determined if the component under test met performance requirements. The test software provided a simple GUI interface to allow operators to record key information and initiate the test process for a set of components. Recorded data was archived in a standard format, with key results stored in JSON format [13] for easy parsing. Test software version control and the use of a git repository was enforced to ensure production testing was reproducible and documented [14]. The Sumatra project tracking tool was integrated into the test software, allowing consistent logging and archiving of all production tests and their outcomes [15].

Each test stand used a commercial personal computer (PC) with 5TB of disk space to run the test software and coordinate testing. All test hardware was controlled by either an FEMB FPGA mezzanine or a WIB, both communicating via the UDP Ethernet interface that was used for real-time diagnostic readout, discussed in Section 1.1.2. Additionally PC USB interfaces were used to control power supplies and function generators. A "server" PC controlled test stand PC configuration through a local network, archived data, and generated summary information and plots used to monitor overall production testing progress. The server possessed 10TB of disk space, sufficient for the data recorded for production tests.

## **2.2 Oscillator Tests**

Two 100 MHz oscillators are assembled on the FEMB FPGA mezzanine as discussed in Section 1.1.1. Each oscillator was tested in LN2 (77 K) to identify components likely to fail during normal cryogenic operation before assembly on the mezzanine. A dedicated test board allowed four oscillators to be tested simultaneously and is shown in Figure 7. Oscillators were placed in individual test sockets by the test stand operator, with power and clock signals transmitted over SMA cables.

The test procedure required the operator to submerge the test board and each oscillator three times in LN2. The three separate cryogenic cycles were necessary to determine whether the oscillators could tolerate repeated cooldowns to cryogenic temperature. While submerged the test script controlled a voltage supply to power the oscillators on-off 100 times. Each time the oscillators were turned on the clock frequency was measured by an oscilloscope and analyzed to check if consistent with 100 MHz. Oscillators that failed to output the correct frequency on any power cycle during any of the three thermal cycles were rejected.

During production testing 700 oscillators were tested by the test stand in total, of which 450 were accepted for installation. The most common oscillator failure was failing to power on correctly when immersed in LN2, while a smaller number produced noisy output. Generally oscillators failed immediately when first powered on at cryogenic temperature. The additional power cycles and immersions were intended to demonstrate that the oscillators that passed the tests were likely to work through the expected operation period of the detector.

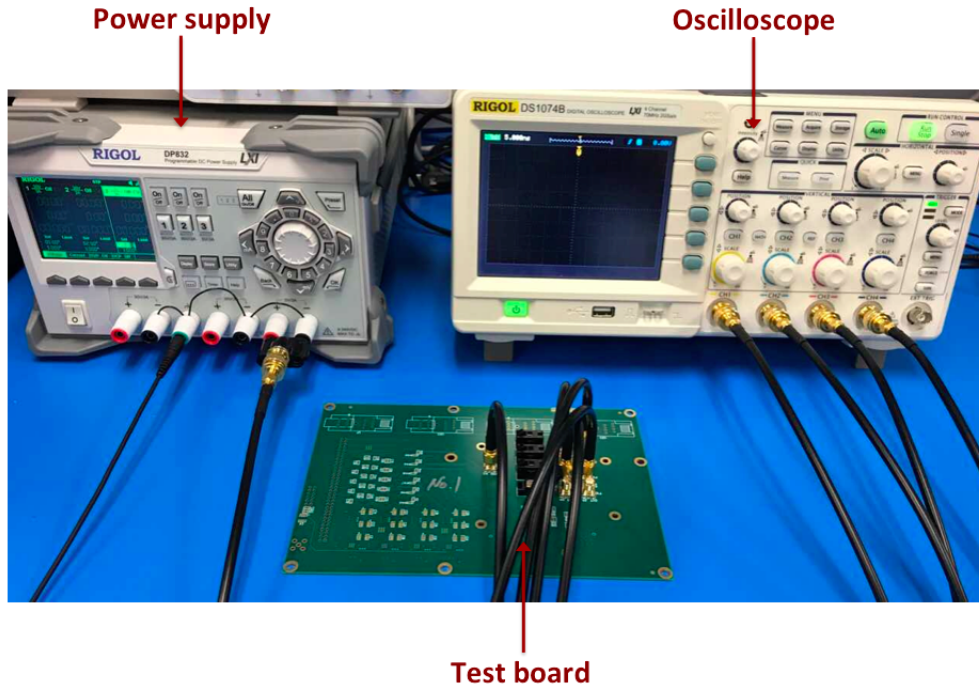


**Figure 7:** Quad-socket oscillator test board with test stand power supply and oscilloscope. The oscillators are placed in the four onboard sockets, and power and signals are transmitted through SMA cables.

### 2.3 Flash Memory Tests



**Figure 8:** Quad-socket flash memory test board, controlled by an FEMB FPGA mezzanine with UDP Ethernet communication to the test PC.

One flash memory device is assembled on the FEMB FPGA mezzanine as discussed in Section 1.1.1. These devices were tested cryogenically to ensure they still functioned correctly before assembly on the mezzanine. A quad-socket test board allowed four devices to be tested simultaneously and

is shown in Figure 8. This test board used an FEMB FPGA mezzanine to control the flash memory erase, read, and write operations, and communicate to the test PC via UDP Ethernet.

During a test the flash memory devices were inserted into the test board sockets by an operator, and then immersed in LN2 while powered off. Care was required to immerse the flash memory chips and not the Ethernet interface transceiver, which would not function correctly at low temperatures. After immersion in LN2 the test script was initiated and the flash memory erase, write, and read back functions were tested in sequence. Erase commands needed to complete within 180 seconds to be identified as successful, and a series of flash memory writes needed to be successfully read back within three attempts.

860 devices were tested in the test stand, of which 190 were accepted for installation. Typical failures were for the flash memory to never report the erase command as successful, or for incorrect data read back following a write command. The high failure rate is not unexpected as the devices were not designed to operate cryogenically.

## **2.4 FE ASIC Tests**

960 FE ASICs are needed for ProtoDUNE-SP. By the end of the QC process 1192 validated FE ASICs were assembled onto production FEMBs, including spares.

### **2.4.1 Warm Screening**

Each FE ASIC was tested at room temperature to avoid assembling FEMBs with defective ASICs. A quad-socket FE ASIC test board was developed to test up to four ASICs at a time, as shown in Figure 9. An FEMB FPGA mezzanine controlled individual ASIC power supply and configuration. Commercial Linear Technology LTC2314 14-bit ADCs digitized and recorded each ASIC channel's amplifier output, sending the digital serialized data to the FPGA which in turn transmitted it via UDP Ethernet to the test PC. An onboard DAC injects square wave signals into the FE ASIC injection capacitor connected to individual FE channel inputs (described in Section 1.1.1). The amplifier electronic response was characterized using the resulting pulses in the digitized waveform, as shown in Figure 10.

To protect the FE ASICs from electrostatic discharge (ESD), operators wore ESD bracelets grounding them to a fixed reference in the lab. Status LEDs on the test boards indicated individual socket power status, reducing the chance of the operator damaging an ASIC by placing it in the test socket while the socket was powered. The test stand script GUI also reduced the chance of damage by directing the operator to place ASICs into the test board when the sockets were unpowered.

After the operator placed up to four FE ASICs in the test board and initiated the test script, each ASIC was power cycled, configured, and data recorded for multiple FE ASIC configurations. Individual channel electronic noise were measured with the RMS of the baseline. Channel gains were measured by varying the magnitude of the DAC driving the injection capacitor and fitting proportional change in average calibration pulse height measurements. This data was analyzed and ASICs rejected if any channel noise and gain measurements were not within acceptable range. These measurements are done for all possible ASIC gain and shaping times, and recording data with pulses provided by the internal FE ASIC or external test board DAC. Different leakage current settings, AC vs DC coupling, and buffer amplifiers were also tested. The full set of tests are defined in Table 2. 1850 FE ASICs were tested at room temperature, with 103 rejected. FE ASICs were



**Figure 9:** Quad-socket FE ASIC test board for room temperature tests. The test board is contained in a stainless steel box, which was closed by the test operator before initiating the test scripts to provide a Faraday cage during ASIC characterization.

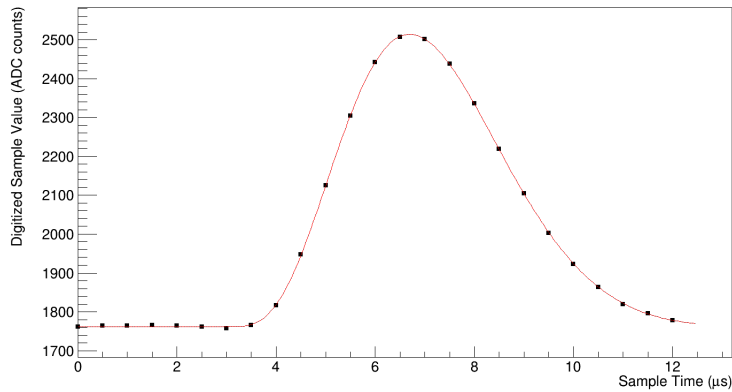


**Figure 10:** An example calibration pulse in the digitized channel waveform, with a fit to the ideal electronics response overlaid for comparison.

generally rejected due to noise or gain measurements outside the acceptable ranges. These ranges were defined as three standard deviations away from the mean of the parameter distribution as measured with a representatively large number of FE ASICs. Some ASICs were also rejected due to individual channels failing to operate correctly.

#### 2.4.2 Cold Screening

The production Analog Motherboards were assembled in batches of ~25, to make the 20 plus spare FEMBs needed to complete a full APA module. For the Analog Motherboards for the first 4 APAs, it was found that ~5% of the FE had to be replaced after cryogenic testing, largely due to the collection-mode baseline drop-out issue discussed in Section 1.1.1 or ESD damage during



Test Type	Number of Tests
ASIC configuration scan with internal ASIC DAC	32
ASIC configuration scan with FPGA DAC	4
Alternative leakage current setting scan	3
Output buffer test	1
AC output test	1

**Table 2:** Summary of pre-amplifier ASIC test process and associated measurements.

assembly. To prevent this rework, FE ASICs for the FEMBs for APAs 5 and 6 were also pre-screened at cryogenic temperature.

A dedicated “stretched” quad-socket cryogenic test board, shown in Figure 11, was developed with extended traces from the FE ASIC sockets to the LTC2314 ADCs and digital control components. This reduced the chance of the commercial ADCs becoming too cold (around -50 °C) during the test to operate correctly. These cryogenic tests determine if the FE ASIC collection channel baseline, nominally at 200 mV, has not dropped below 100 mV due to the packaging stress, so that the channel is safely above the baseline range with poor channel performance, and could observe the injection capacitor pulses. 320 FE ASICs are needed for APA5-6 FEMBs. 550 ASICs were cryogenically tested, and 368 accepted. The majority of the ASICs initially rejected were due to failures of the test sockets; upon retest of the rejected FE ASICs a failure rate of ~4% was observed, consistent with the FE failure rate when cryogenically testing the FEMBs.

The commercial test sockets were not designed to operate at cryogenic temperature and would eventually become unable to make stable low-impedance contact to the ASIC pins due to socket deformation from repeated thermal cycles.

## 2.5 ADC ASIC Tests and Selection

To optimize detector performance, a large number of ADC ASICs were tested at room and cryogenic temperature. The best performing ASICs were then selected for assembly onto the Analog Motherboards. A single-socket ADC ASIC test board was designed to test one ASIC at a time, as shown in Figure 12. An FEMB FPGA mezzanine controls the ADC ASIC and reads out the two serial data streams, which it sends to the test PC via the UDP Ethernet interface. A function generator controlled by the Python test script provides input signals through a LEMO cable to the test board.

To test a single ADC ASIC the operator places it into the chip socket while the test board is powered off. The operator follows the ESD protection protocol described in Section 2.4.1. At this point the warm testing process is initiated through the GUI, which checks for basic functionality including whether the ASIC can be powered on, configured and the digital data stream synchronized correctly with respect to the FPGA digital logic. If this is successful a sinusoidal wave signal produced by the function generator is injected into all ADC ASIC channels and the resulting digitized waveforms displayed in real-time in a GUI window as shown in Figure 13. This waveform display provides visual confirmation to the operator that the test setup is working and the ADC ASIC is functioning correctly at room temperature. At this point the ADC ASIC is submerged into LN2 while the operator observes the real-time sinusoidal waveforms. Care was taken not immerse the Ethernet





**Figure 11:** Quad-socket FE ASIC test board for cryogenic testing with three of four ASIC sockets installed. The additional distance between the ASICs and digital electronics improved ADC reliability by preventing them from becoming too cold to operate correctly during a cryogenic test.

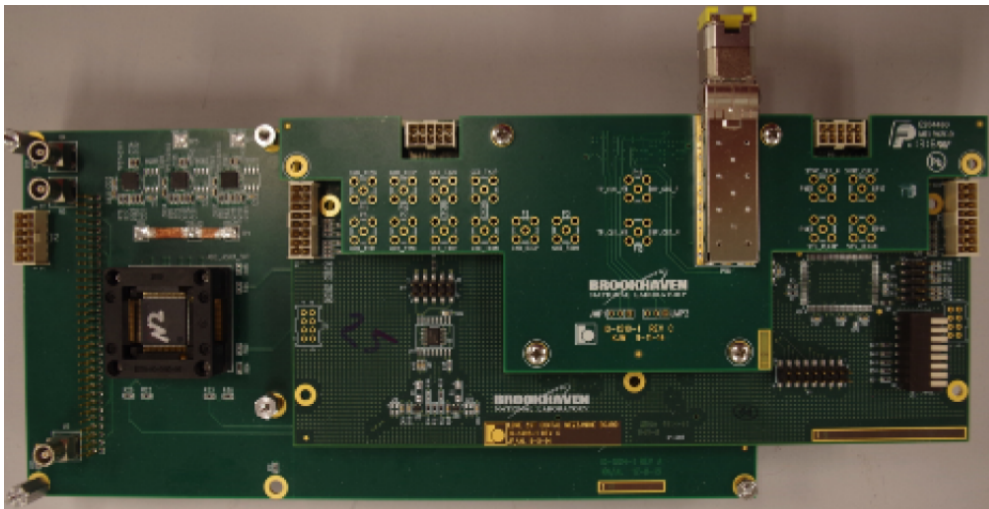


**Figure 12:** Single-socket ADC ASIC test board, with ADC ASIC installed in socket.

interface transceiver. The real-time waveform display provided crucial feedback to the operator during the immersion process as to whether the ADC channels functioned properly: if a channel failed, the test was ended before the test script was launched.

Once fully submerged the operator started the cryogenic ADC ASIC test script, the stages of which are:

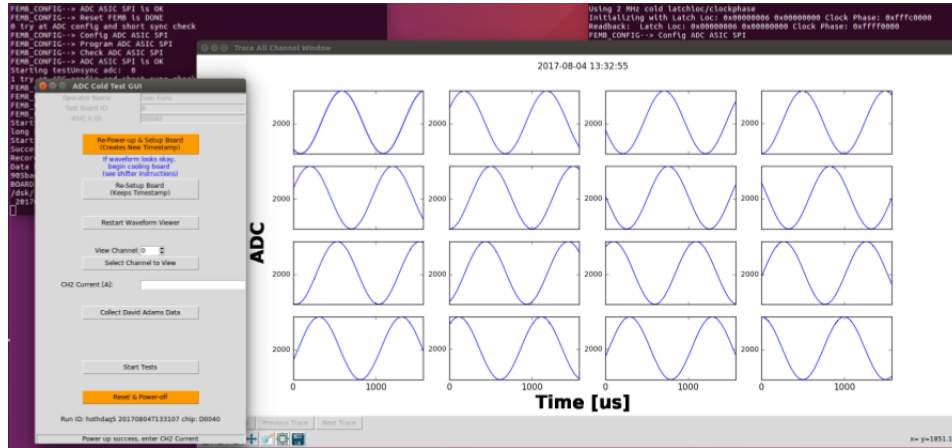


**Figure 13:** Single-socket ADC test GUI and sinusoidal waveform display, indicating that the ADC readout is working correctly at room temperature prior to submersion in LN2.

- Injecting a long ramp signal into the ADC channel inputs with magnitude sufficient to cover the full ADC dynamic range. The digitized waveform of the long ramp signal was used to estimate ADC linearity and other parameters, such as input voltage range and including the sticky codes discussed in Section 1.1.1, from which an overall ADC quality metric was derived.
- A series of functionality tests identified ADCs that failed to operate correctly cryogenically, including verifying the ASIC could be power cycled, configured, and record data at cryogenic temperature for all 16 input channels.
- Measurements of ADC integral and differential nonlinearity (INL and DNL) and dynamic range were also used to reject underperforming ASICs.
- Disconnected or malfunctioning channels were also detected, as were channels experiencing a higher than average incidence of the sticky code error.

These tests were performed for four sets of ADC ASIC settings, where the source of ADC clock and control signals was switched between the ADC ASIC internal logic and logic provided by the FPGA, and also switching between 1MHz and 2MHz sampling rates. After these tests finished summary plots were automatically generated for the operator to review as shown in Figure 14 indicating whether the ADC ASIC had been rejected.

Using this procedure 3680 ADC ASICs were tested, of which 271 were rejected outright. The remaining ADC ASICs were ranked in terms of performance based on the long ramp signal data, and the 1192 (~30%) best-performing ASICs were selected for assembly. ADC ASICs were typically rejected for an inability to correctly synchronize its output serial data stream with the FPGA digital logic. Poor performance or malfunction of one or more channels were also reasons for rejecting ADCs.

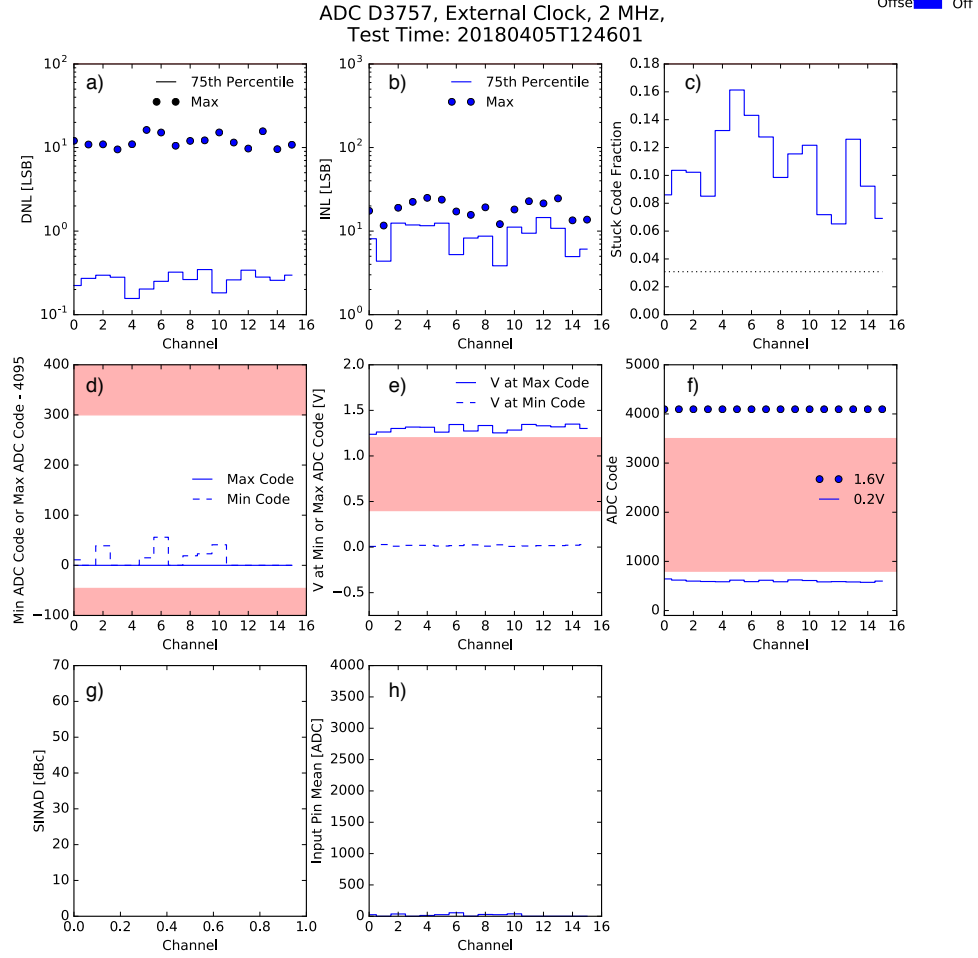


**Figure 14:** Single-socket ADC test summary plot, showing the results of the cryogenic temperature ADC ASIC functionality and performance tests. Plotted results show channel-specific measurements of a) DNL, b) INL, c) fraction of samples with the stuck code error, d) minimum and maximum ADC codes within the ADC linear region, e) input voltage dynamic range measurement, f) average digitized sample code for 0.2 V and 1.6 V input voltages, g) signal-to-noise and distortion ratio, h) average digitized sample code for disconnected ADC input. One summary plot was produced for each of the four ADC operating modes evaluated during the cryogenic test.

## 2.6 Warm Interface Electronics Tests

Dedicated test stands were not constructed for the warm interface electronics components (WIB, PTB, PTC, and flange PCB), due to the relatively low number of components and the less challenging room temperature operating requirement. However the components used in ProtoDUNE-SP also underwent a series of QC tests at BNL after assembly to ensure they functioned correctly when integrated and reading out FEMBs. Additional tests were performed during installation as described in Section 3.

## 2.7 FEMB and CE Box Tests

Following individual component testing, FEMBs are assembled with components that passed previous tests. 120 FEMBs are needed to fully instrument all ProtoDUNE-SP APAs; including spares, 149 FEMBs were assembled in the production run. Assembled FEMBs then underwent pre-testing to verify basic functionality of the FPGA and ASICs, and identify whether any rework was required. Successfully pre-tested FEMBs were then mounted within a "CE box" as shown in Figure 15, and fitted with a cold cable bundle and input pin adapter. The CE Box provides mechanical support of the cables, protection of the FEMB components, and hardware for attaching to the APA frame. This assembly was then tested as a unit at room and cryogenic temperature to fully evaluate functionality and performance. Critically these tests were performed using the WIB UDP Ethernet readout used for real-time diagnostic commissioning of the detector, validating the complete CE readout chain from FE input to WIB output for every CE Box and set of cold cables.

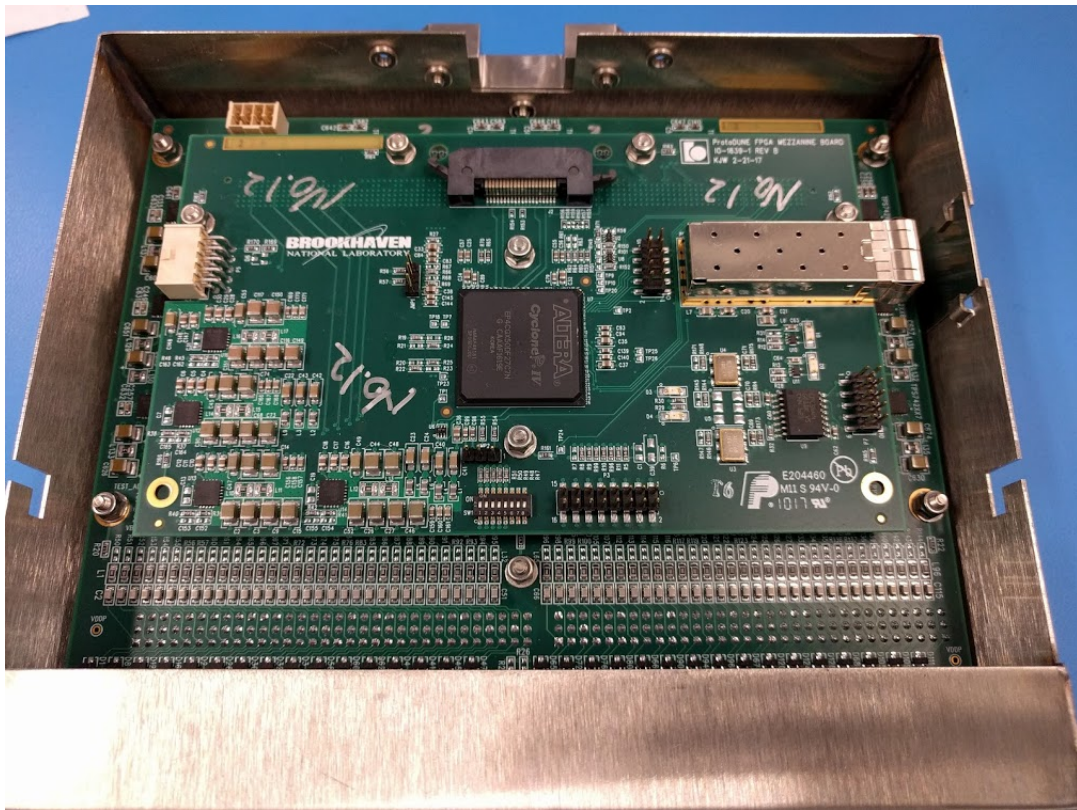


**Figure 15:** Assembled FEMB integrated into a cold electronic box, prior to production testing.

The initial FEMB test stand setup is shown in Figure 16. The operator installed the CE Box in a wire mesh bucket that provided shielding and support during testing, and then initiated room temperature and cryogenic tests through a GUI. The room temperature and cryogenic tests were identical aside from different configurations needed to synchronize the ADCs to the FPGA for room temperature and cryogenic operation as discussed in Section 2.5.

Functionality tests included verifying the ability to power up and configure correctly, as well as checks that the voltage current draws on the power lines from the WIB to the FEMB are normal.



Semi-realistic ENC measurements were obtained by fitting two “toy TPC” PCB that provide 150 pF input capacitance for every channel, which simulates the input capacitance expected for a DUNE 7.5 meter APA wire.

Channel gain measurements were obtained similarly to the FE ASIC tests discussed in Section 2.4.1, where both the internal FE and FPGA DACs were connected to the FE ASIC injection capacitor and varied in size while the corresponding changes in average calibration pulse heights were measured. The resulting channel ENC and gain measurements obtained with different ASIC configurations were used to reject FEMBs with malfunctioning components or unacceptable performance.



**Figure 16:** The FEMB production test stand, showing LN2 dewar, mesh bucket containing the CE Box inside the dewar, cold cables and WIB board. The code cables are held inside another wire mesh bucket outside the dewar during the test to minimize electronic noise pickup.

After the room temperature tests, the CE Box was slowly immersed into LN2 and the test script initiated again for the cryogenic tests. At the end of each of the room temperature and cryogenic test process a summary document was automatically generated as shown in Figure 17. This document summarized the tests performed and board performance, and was used to identify and reject boards with malfunctioning channels, excessive electronic noise or failure to function correctly.

Of the 149 FEMB and CE Box production assemblies tested, ~4% required expert technician rework of the FEMB, and four were rejected due to unrepairable excessive ENC or poor performance in one or more channels. FEMBs that passed these final QC tests were delivered to CERN for acceptance testing and installation, as described in Section 3.

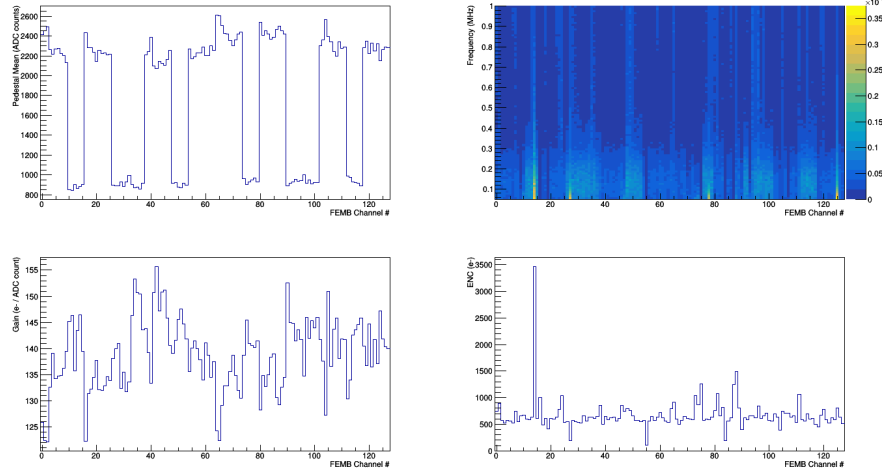
### protoDUNE FEMB QC Summary: CE Box 5

Timestamp: 20170814T182216      Tested by: Brian Kirby      Temperature: CT  
 Analog MB ID: 2      FPGA Mezz ID: 17  
 FE ASICs: 220,221,225,227,140,230,231,232  
 ADC ASICs: 97,90,65,53,118,81,22,385

Average ENC measured with internal pulser (electrons)

	0.5 us	1 us	2 us	3 us
14 mV/fC	1083	773	671	666
25 mV/fC	994	661	626	630

Gain/ENC Measurement: Gain = 14 mV/fC, Shaping Time = 1 us, Internal Pulser



FEMB power cycled 5 times at beginning of data collection with no failure.

Current Monitoring:

Nominal Voltage	4.2 V	3 V	2.5 V	1.5 V	5 V
Voltage (V):	4.06	2.89	2.40	1.44	4.80
Current (A):	0.06	0.39	1.10	0.48	0.01

Data stored on hothdaq1:

/dsk1/data/oper/femb/wib\_sbnd\_v109\_femb\_protodune\_v308/20170814T182216

Position on WIB for test: 1

**Figure 17:** Example FEMB QC test summary document, which summarizes results of the power cycle test, current draw, and average ENC measurements used to evaluate FEMB performance.

## 2.8 Cryogenic Test System

An automated Cryogenic Test System (CTS) was introduced to the FEMB quality control tests and used to test the final ~50% of the production CE Boxes. The CTS with a CE Box under test is shown in Figure 18. In addition to testing CE Boxes, the CTS was designed to immerse the FE ASICs in the stretched quad-socket test board shown in Figure 11. Two CTS were used to cold screen the FE ASICs for APA5-6, as discussed in Section 2.4.2. A total of three CTS were used for



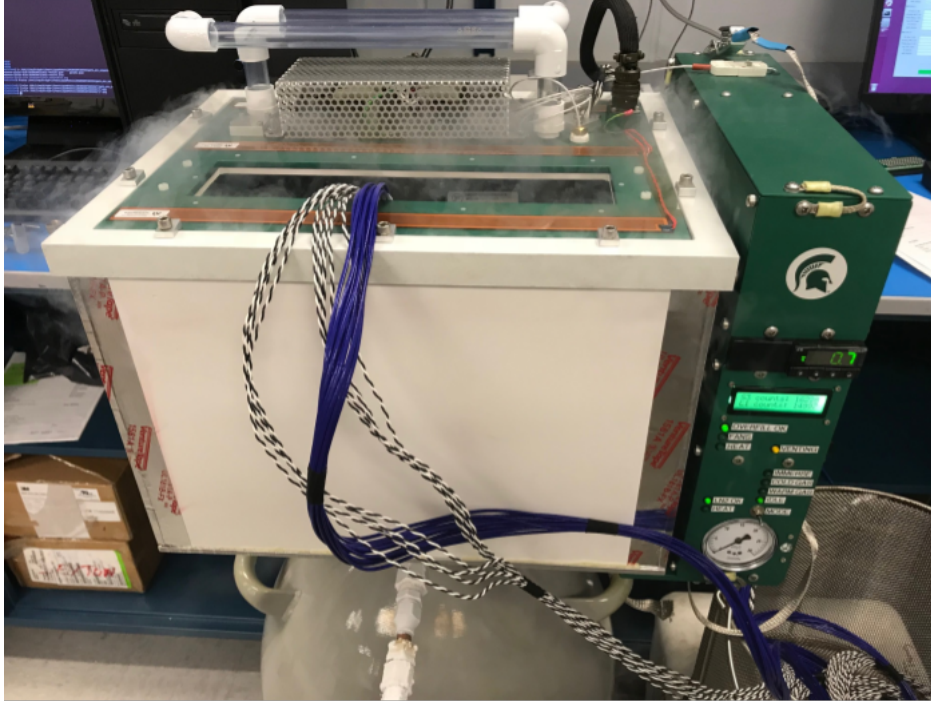


**Figure 18:** A production CE Box held within the CTS for a quality control test. The CTS automates the LN2 immersion and warming back to room temperature processes.

the final production QC tests at BNL.

The CTS automates the immersion of components in LN2 for cryogenic testing purposes, as well as the subsequent warming back to room temperature. A key improvement over the open-top dewar test stand is that the CTS flushes the chamber holding the component under test with cold nitrogen gas before immersion, removing any humidity that might condense on the component. Similarly after the QC test is complete the CTS warms the chamber in nitrogen gas, reducing the chance of water condensation and protecting the components under test. The CTS did not require altering the production tests: when the FE ASICs or FEMB were immersed in the CTS, exactly the same GUI-controlled test software discussed in Sections 2.4.2 and 2.7 was used to run the production QC tests. ENC measurements were  $\sim 10\%$  higher for tests performed in the CTS over the open-top dewar, due to the operation of liquid level sensors in the CTS. This did not affect identification of malfunctioning or under-performing FE ASICs or FEMBs.

## 2.9 Summary and Lessons for Future LArTPC Experiments

A summary of the QC test results for all components is shown in Table 3. The relatively low rejection rate of FEMBs was a major achievement and in large part due to pre-screening of individual components. Reworking already assembled FEMBs to replace a failing component requires an expert technician and can damage other components; minimizing the rejection rate reduces this risk.

The ProtoDUNE-SP QC testing effort provided a great deal of experience that can be applied to future LArTPC electronic productions. One shortcoming in test design was the failure to test

FE ASICs with an extended test signal to simulate a long ionization charge distribution. This is a common type of charge distribution within a LArTPC and the associated electronics response should have been evaluated. Simplification of the GUI software and automation of the testing process and component pre-testing helped the QC test stands process the electronics production in a timely manner, allowing non-expert operators to be quickly trained and run the test stands in shifts, and is an approach that should be carried forward to future efforts.

Component	Number Tested	Rejection Rate
100MHz Oscillators	700	35.7%
Flash Memory	860	77.9%
Pre-amplifier ASIC (warm)	1850	5.6%
Pre-amplifier ASIC (cold)	168	4.2%
ADC ASIC	3680	14.6%
FEMB	149	2.7%

**Table 3:** Summary of ProtoDUNE-SP electronic component QC tests.

### 3 Installation

The following flow chart (Figure 19) shows all the testing steps performed separately at BNL and CERN on all the different CE components. In the following section will be described the installation and activation procedures carried out at CERN. As shown in the plot, the installation at CERN included three different steps. The first one (CE installation) includes a set of checkout test performed on the CE boxes from their delivery at CERN to their installation on the APA. Those tests, along with the Cold Box test described in Section 3.2, allowed to verify the functionality of all readout channels and the ENC levels before inserting the APAs into the cryostat. The last set of test, allowed to verify and maintain the electronics performance during the detector commissioning where the installation of other subsystem may affect the electronics functionality.

#### 3.1 Reception test and installation

Once delivered to CERN, the CE Boxes were tested several times throughout the installation steps. A first reception test was performed at room temperature on all the CE Boxes before installation on the APA. To protect against ESD damage to the FEMBs, the CE Boxes were shipped with the cold cables detached from the electronics. Once the cold LV and data cables were re-assembled, the shorting caps were removed and the CE Box was connected to a test setup consisting of a readout PC connected via Ethernet to a WIB, and an adapter board simulating the WIEC connection. Two 150 pF toy TPCs, described in Section 2.7, were connected to the CE Box inputs to simulate the APA capacitance.

ENC was measured on all channels for all FE ASIC gain and shaping time settings. The pulse response of each FEMB was checked by injecting bipolar pulses from the FE ASIC calibration circuit described in Section 1.1.1. Through averaging calibration response over many pulses, functionality of all readout channels was verified. CE Boxes were only accepted for APA installation if all

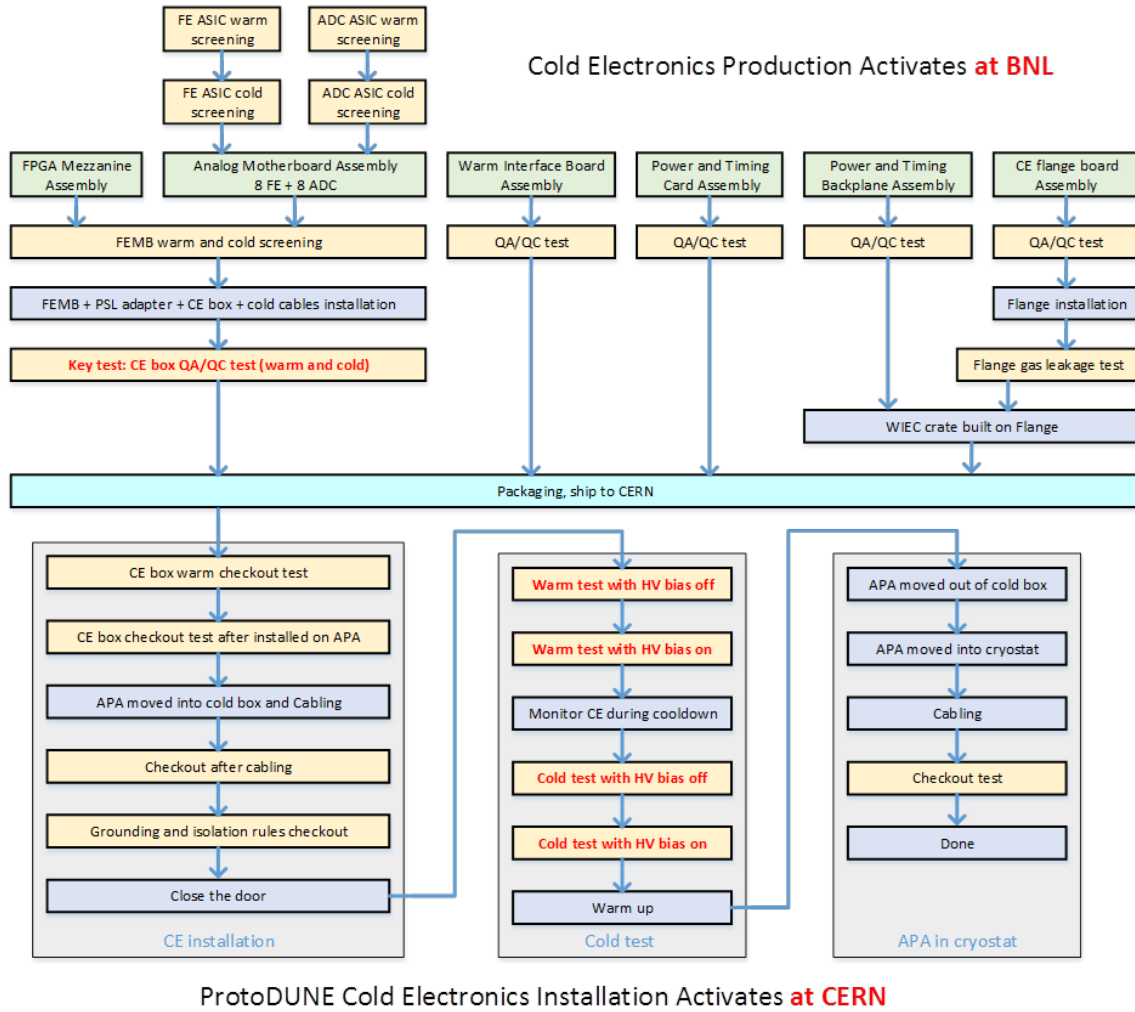


**Figure 19:** Flow chart showing the different stages for the cold electronics production at BNL and installation and activation at CERN.

128 channels were functional and observed ENC levels typical for room temperature operation: 1000 – 1500  $e^-$ .

The same test was repeated on each CE Box after the installation on the APA and for four CE Boxes in a group connected to the same WIB after cabling. CE Boxes with any loss of channel functionality after installation were removed from the APA and replaced with a spare CE Box. Several CE Box failures were observed at these stages: 3 at the reception test, one after the installation, and none after the cabling. In Table 4, a detailed summary of CE Box failure at these and the following testing stages is shown. One further CE Box failure occurred during the detector filling which is described in Section 4.2.

A data cable connector failure, which resulted in loss of communication between the WIB and the CE Box, was the most common issue, especially during the Cold Box test at RT and during the cooldown described in Section 3.2. Microscope analysis of a damaged FEMB performed at BNL revealed some micro-cracks on the connector welding to the FEMB FPGA mezzanine, causing the

APA number	CE Box ID	Failure description	Testing stage
1	9	1 dead FE channel at RT	QC test at BNL Installation Installation
	20	LV return wire cut during cabling on APA	
	24	3 dead FE channels at RT	
2	39	Data cable connector failed during cooldown	Cold Box Test
3	69	1 dead FE channel at RT	Reception test
	49	Data cable connector failed at RT	Cold Box Test
	18	Data cable connector failed at RT	Cold Box Test
	22	1 FE ASIC (16 channels) failed during cooldown	Cold Box Test
	75	Data cable connector failed at RT	Cold Box Test
4	91	1 dead FE channel at RT	Reception test
	85	Data cable connector failed during cold test	Cold Box Test
5	122	2 links failed during warm test	Cold Box Test
	123	Data cable connector failed at RT	Cold Box Test
	106	Data cable connector failed at RT	Cold Box Test
6	112	Data cable connector failed at RT	Cryostat checkout

**Table 4:** Detailed summary of the CE Box failure at different testing stages during the TPC installation and commissioning.

connector to partially separate from the PCB. Further testing at BNL confirmed that this failure could be induced through a combination of mechanical and thermal stress. For this reason, a new data connector design for the next FEMB version is currently under review.

### 3.2 Cold Box Integration Test

In order to evaluate fully-instrumented APA performance at cryogenic temperature, a Cold Box was built for integration testing at CERN (Figure 20). The integration test included a full production signal feed-through assembly and WIEC, described in Section 1.1.2, containing production PTB, PTC, and five WIBs. This allows a vertical slice test of all APA wires, CE readout, and photon detectors (described in Chapter 2.7 of [4]) on production APAs before insertion into the cryostat. The CE readout through optical fibers from the WIBs allows a real-time study of the detector performance in Cold Box tests, independent from the full DAQ readout. Seven temperature sensors installed on one side of the APA allows continuous monitoring of the temperature inside the Cold Box and the temperature gradient between the bottom and the top of the APA where the CE is installed. The APAs were cooled down over an approximately 24 hour period to  $\sim 150$  K at the CE by injecting cold nitrogen gas from the top of the cold box.

The ENC performance was evaluated first at room temperature and during all the cold test stages (cool down, stable cold temperature, and warm up). In Figure 21 the ENC with FE gain of 25 mV/fC and shaping time  $2\ \mu\text{s}$  of the induction planes (blue and red) and collection plane (green) for APA2 are shown as a function of time; the temperature values corresponding to the several temperature sensors (orange) installed on one APA side are also shown. At room temperature, the ENC is around  $1200\ \text{e}^-$  for the induction planes and  $1100\ \text{e}^-$  for the collection plane. At the lowest temperature achievable by the Cold Box facility, the ENC reaches a minimum value at  $\sim 500\ \text{e}^-$  for the induction planes and  $\sim 400\ \text{e}^-$  for the collection plane, matching to the ENC projection presented in [7] after correction for the wires in gaseous rather than liquid nitrogen. In Figure 22, a more detailed comparison between the ENC at warm and cold temperature is shown for FE gain values 14 and 25 mV/fC as a function of shaping time, demonstrating the advantages of the CMOS technology at cryogenic temperatures.



**Figure 20:** Picture of the Cold Box facility for APA integration test. In the picture, the APA-assembly (APA+CE system+PD system) is ready to be inserted into the cold box. On top of the APA you can also see 10 out of 20 installed CE boxes.

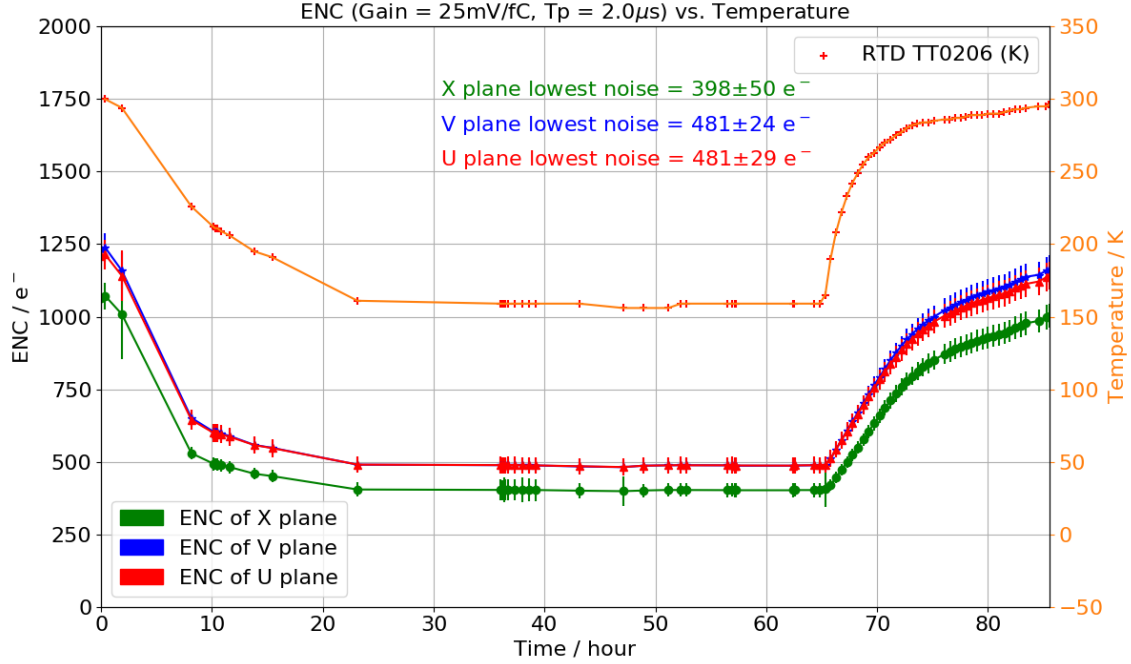


**Figure 21:** ENC performance in electrons of the APA+CE during the Cold Box test as a function of time; red/blue are the collection (U/V) wires, green are the induction (X) wires. The temperature is measured by RTD sensors installed on one side of the APA; the orange curve is the RTD at the level nearest the CE Boxes.

#### 4 Commissioning

In April 2018, the TPC installation was complete and all its components were positioned inside the cryostat and commissioning activities started in order to be ready for the first detector data beam run on September 2018. Commissioning of the detector included fixing the APA, CPA, and field cage end walls in their final position, installing the high voltage cup and feedthrough and all the cryo-instrumentation, cameras, LEDs, purity monitors, and temperature sensors.

Electronics commissioning comprised attaching the cold LV and data cables to the CE signal feed-throughs, Warm Interface Electronics installation, installing the optical fibers and checking the CE-to-DAQ-system connection. Before starting the cabling at the WIEC, the functionality of all FEMB channels was checked again by using the stand-alone WIB test setup and identical metrics to those described in Section 3. No variations were found from the last test before moving the APAs inside the cryostat. Finally, as each set of four CE Boxes were cabled to the signal feed-throughs, the corresponding WIB was inserted in the WIEC and an identical set of tests were run; after all cables and WIBs were installed, one FE channel was not responding to the FE calibration pulser at room temperature (0.0065%).

Throughout the detector commissioning, the baseline, RMS, and calibration pulser response of the CE have been periodically monitored by the WIB diagnostic readout. A significant increase was



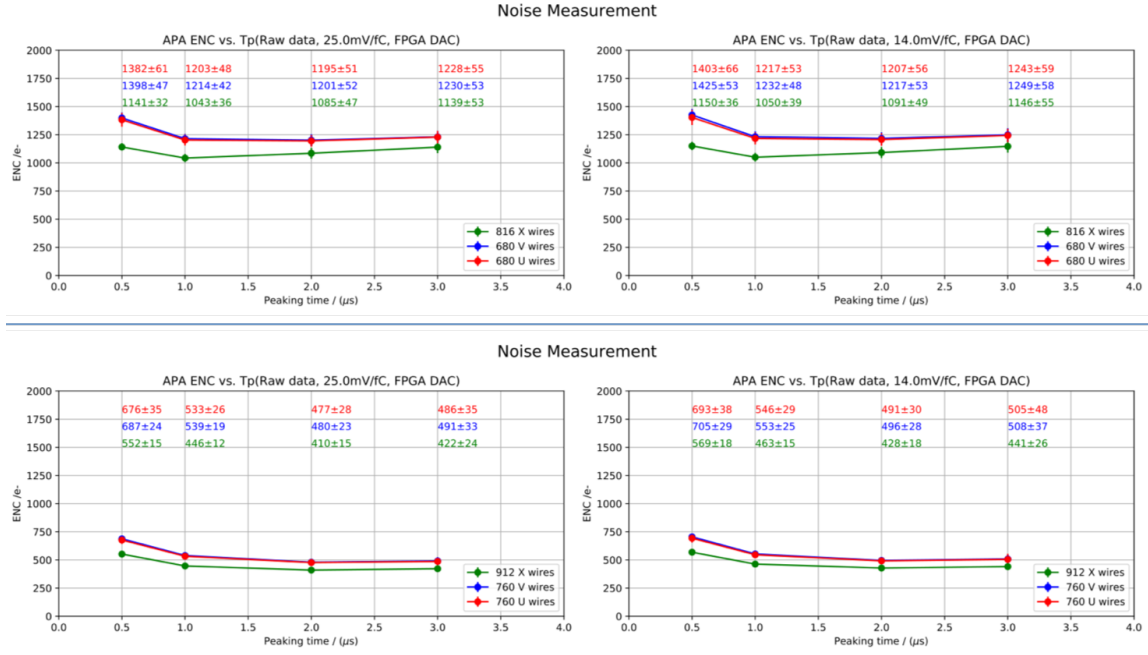


**Figure 22:** Comparison between average ENC (e<sup>-</sup>) at warm (*top*) and cold (*bottom*) temperature for two different gain values (25 mV/fC *left*, 14 mV/fC *right*): red/blue are the collection (U/V) wires, green are the induction (X) wires. The overall lower ENC for the X wires is due to the shorter wire length of 6 m compared to the ~7.5 m U/V wires.

observed in RMS after the installation of LEDs and cameras, especially on the closest APAs (APA4 and APA6). A series of tests on APA4 showed that the noise was induced by the 12V power supplies installed for the LEDs and cameras. Even without powering on the LEDs and cameras (supply on, setting 0V), the noise was still there transmitted to the detector ground by the return wire. The solution was to replace the 12V power supplies with a linear DC LV supply. Figure 23 shows the RMS observed on APA4 before and after the replacement of the power supply. In both cases, cameras were on during the test. However, after power supply replacement, two peaks at ~500 and 600 kHz were still observable with a Fast Fourier Transform (FFT) analysis in the frequency domain due to LEDs and cameras. The remaining noise after replacement has been filtered at the offline data analysis stage.

In August 2018, detector commissioning was completed and the cryogenic group started the purging and filling procedures. In September 2018, the detector was fully filled with LAr and ready for the activation procedure.

#### 4.1 Electronics Performance

Table 5 shows a detailed summary of the TPC channels performance measured in several tests during the detector activation. The last test is September 23 when the nominal cathode drift voltage value of -180 kV was reached and detector was fully operating.

As of August 2019, after ~7 weeks of beam data-taking and ~8 months of cosmic rays data-taking, 42 channels are found to be non-operational, with 99.7% of 15,360 TPC channels in total working

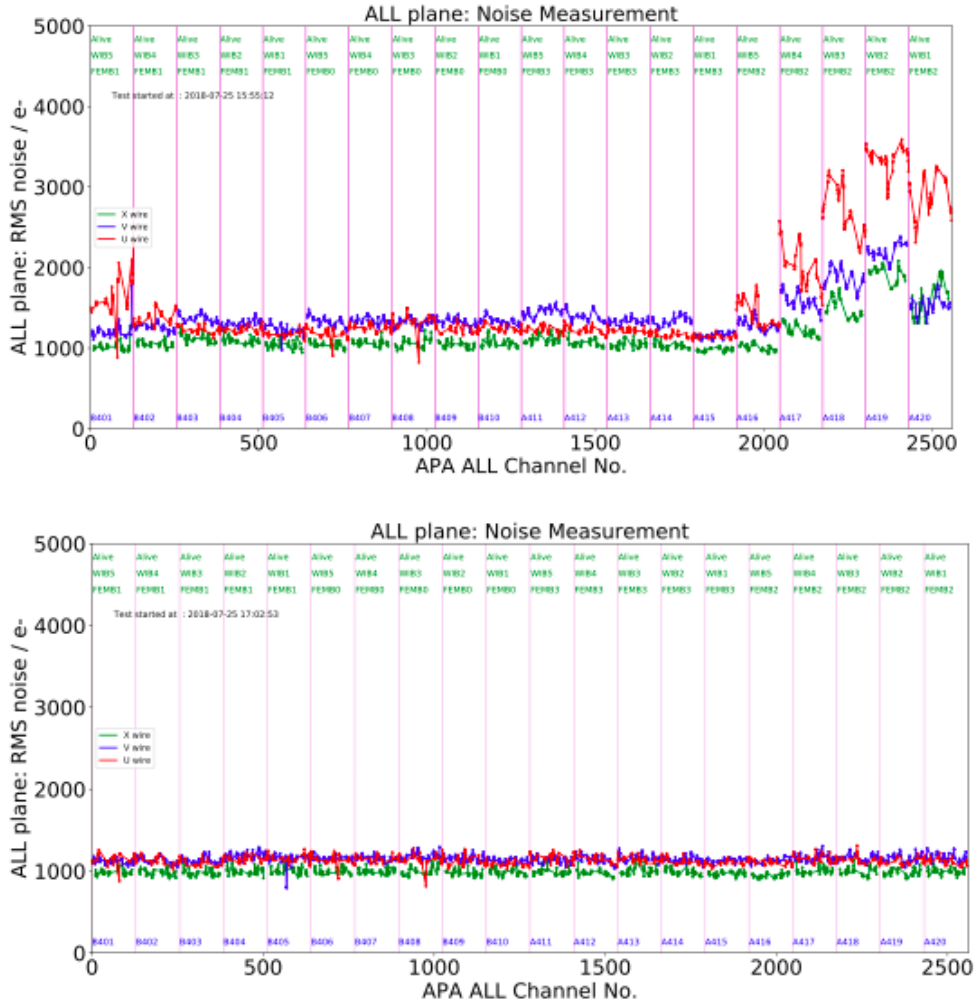


**Figure 23:** Comparison between RMS on APA4 before (*top*) and after (*bottom*) the replacement of 12V power supplies for LEDs and cameras with a linear DC LV supply.

properly. Of those 42 channels, 38 are missing or disconnected wire candidates and 4 are non-responsive to the FE calibration pulser. 93% of the TPC channels are working with excellent noise performance ( $ENC < 800e^-$ ), well below the CE design requirements for the DUNE FD. For the remaining 7%, the abnormally high RMS has been mostly correlated in further studies at CERN to either the drift HV power supply operation or the TPC instrumentation, as already observed during the commissioning stage. In Figure 24, the overall ENC observed on a standard checkout run (RUN 5102) is shown for the three wires planes.

In Figure 25 is shown the FEMB inverted gain comparison between the beginning of the full-detector operations (Sep 2018) and one year later (Dec 2019). The measured gain shift is around 0.13% and 0.4% RMS, with an excellent agreement between 2018 and 2019 (around 0.01% shift with 0.3% RMS). In Figure 26, is shown the comparison channel by channel of the inverted gain between the same two runs.

<b>Test ID</b>	# 1	#5	#9	#11	#13	#15	#18	#35	
<b>Date</b>	9/13	9/14	9/16	9/16	9/17	9/19	9/20	9/23	
<b>HV status</b>	off	-120kV	off	off	off	off	-160kV	-180kV	
<b>Not Working Ch.</b>	112	112	112	112	112	0	0	0	ADC sync error
	13	40	0	12	12	6	0	0	FE with start-up
	0	3	2	2	2	2	2	4	Inactive FE channels
	6	4	4	4	4	4	2	2	FE gain < 180 e <sup>-</sup> /ADC
	48	52	48	46	48	46	59	45	Non-removable stuck code
	41	38	37	38	36	37	39	38	Open connection
	2	0	0	0	0	0	1	3	ENC > 2000 e <sup>-</sup>
	295	348	334	330	292	318	405	386	2000 e <sup>-</sup> < ENC > 1000 e <sup>-</sup>
	446	466	451	463	457	442	655	627	1000 e <sup>-</sup> < ENC > 800 e <sup>-</sup>
<b>Good Ch. (ENC &lt; 800 e<sup>-</sup>)</b>	14397	14297	14372	14353	14397	14377	14179	14259	
<b>Active FE Ch.</b>	15229	15201	15242	15230	15230	15220	15338	15354	
<b>Active TPC Ch.</b>	15188	15163	15205	15192	15194	15183	15299	15318	

**Table 5:** Performance of TPC channels measured throughout detector activation. The last column shows how CE failures have been classified. Failures are listed from high to low priority.

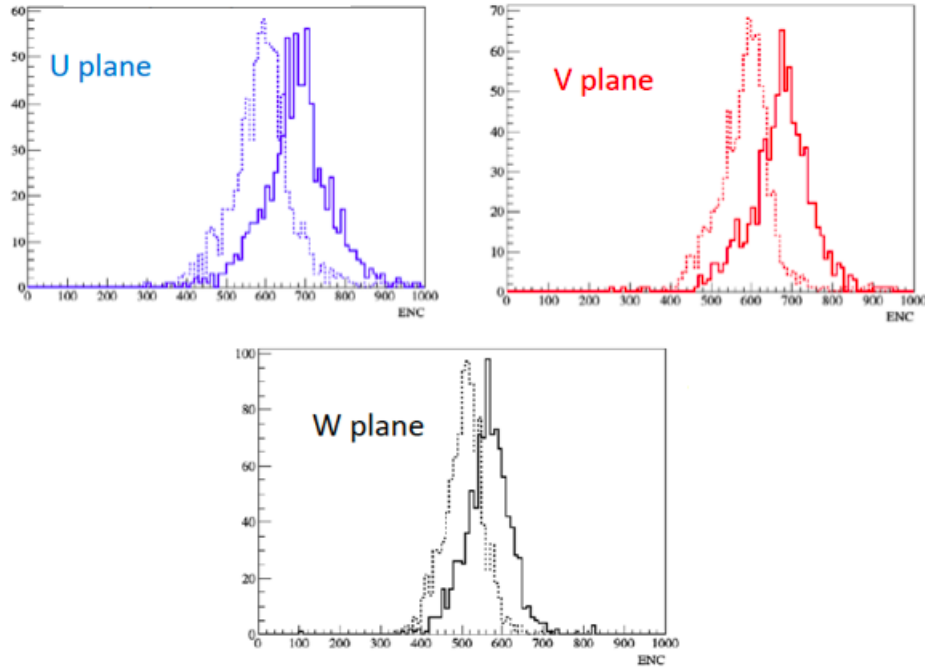


**Figure 24:** Overall ENC observed on RUN 5102 on the three wires planes. For each plot, the ENC before (dashed line) and after (solid line) the offline noise filtering is shown.

## 4.2 Clock failure on FEMB302

During detector filling, communication was lost to one CE Box on APA3. The failure mode for this CE Box was similar enough to the ones in the Cold Box to suggest an FEMB data connector failure. However, a detailed check with the WIB Ethernet diagnostic readout showed that the FEMB link

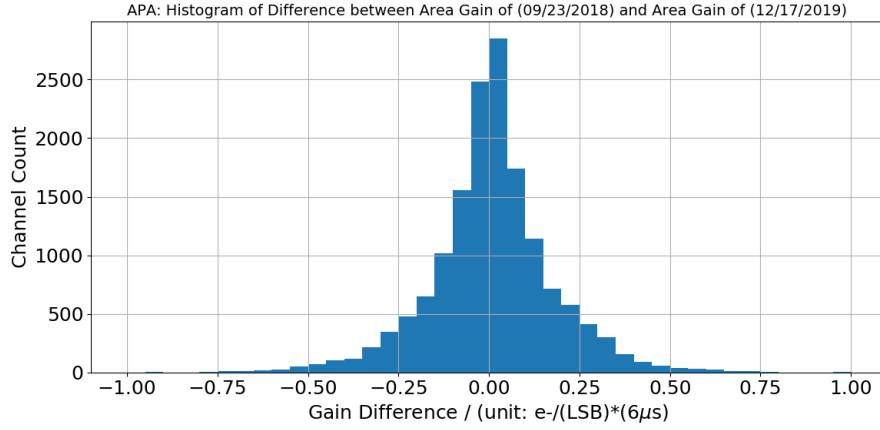


**Figure 25:** FEMB inverted gain difference between the beginning of the full-detector operations (Sep 2018) and one year later (Dec 2019)

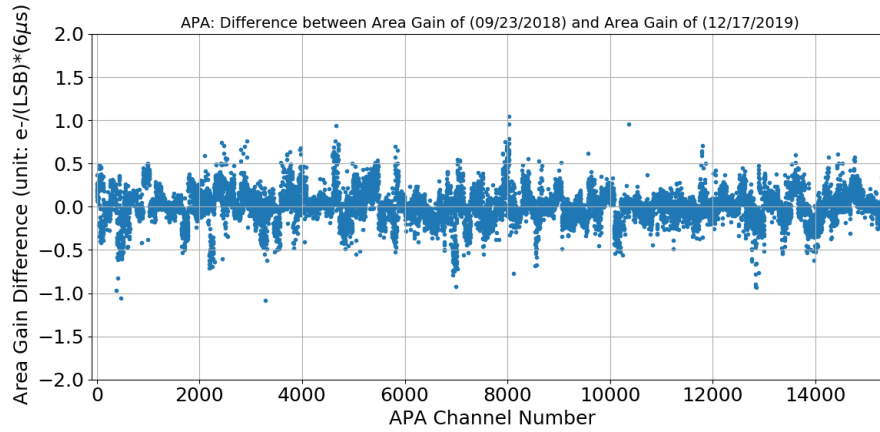


**Figure 26:** Channel by channel difference of the inverted gain between the beginning of the full-detector operations (Sep 2018) and one year later (Dec 2019)

connection was still active, suggesting that only the system clock pin on the data connector was actually broken causing a communication interruption between WIB and FEMB. To recover the FEMB, a new firmware version for the FEMB FPGA that bypassed the system clock and used the backup oscillators discussed in Sections 1.1.1 and 2.2 as the FEMB clock was programmed over the backup JTAG links. The unavailability of the system clock caused the ADC digitization on all 128 FEMB channels to be asynchronous with the rest of the CE system. To correct this, data filtering is performed offline using track candidates to correct synchronization errors and restore the original shape of the track. Figure 27 shows an example of a particle track before and after the offline correction.

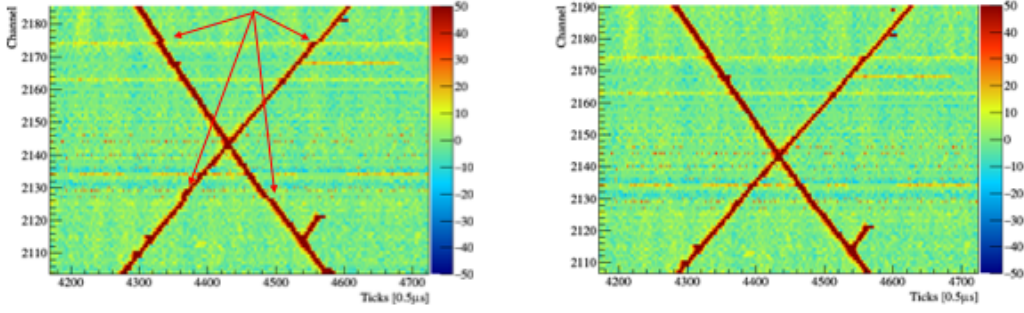


**Figure 27:** Example of a particle track before (*left*) and after (*right*) the offline data filtering. Synchronization errors on the track (pointed out by the arrows on the left) have been fixed restoring the original track shape.

## 5 Conclusion

The protoDUNE-SP detector at the CERN Neutrino Platform has been a successful validation of the Cold Electronics LArTPC readout system for the DUNE Far Detector. The CE system contains all the electronics necessary to amplify, shape, digitize, and transmit the TPC wire data out of the cryostat to the DAQ system while operating at cryogenic temperatures (77 – 89K). This enables readout of large LArTPC detectors at the very low noise level of  $ENC < 1000 e^-$  and separation of the electronics and TPC designs. Additionally the CE includes warm interface electronics, which provide local power control and real-time diagnostic readout at the cryostat, which was used to perform the validation and integration tests from individual CE Boxes, to fully integrated APAs in the Cold Box, to the completed TPC inside the cryostat.

120 CE Boxes were installed on 6 APAs by April 2018 for 15,360 total TPC readout channels. These CE Boxes were selected for installation from a comprehensive QC testing effort. This QC effort also led to excellent CE performance during the installation and commissioning phases of detector operation, with 99.7% of TPC channels active and 92.8% operating at very low levels of ENC. The performance of the TPC readout was monitored with the diagnostic readout during the detector activation phase leading up to physics data-taking in September 2018 and found only 4 channels became inactive in the CE during this period. Currently protoDUNE-SP is taking cosmic ray data with very stable performance from the CE.

## Acknowledgments

The work described in this paper would not have been possible without a large number of collaborating institutions from the DUNE Collaboration, who provided shift leaders and shift operators for all of the quality control tests at BNL and who contributed to the installation and commissioning work at CERN. In particular we would like to thank: Boston University, University of California at Davis, CERN, University of Cincinnati, Chung-Ahn University, Colorado State University, Comsewogue High School, Fermi National Accelerator Laboratory, University of Florida, University of Houston, Iowa State University, Kansas State University, Louisiana State University, Michigan

State University, Stony Brook University, University of Texas (Arlington), Tsinghua University, and the US Department of Energy Science Undergraduates Laboratory Internships program. We acknowledge the support from DOE (Department of Energy) USA. We would also like to specifically thank Roberto Acciari, Flavio Cavanna, Karol Henessey, Giovanna Lehmann, Regina Ramika, Filippo Resnati, and Christos Touramanis for their leadership during the preparation, installation, and commissioning of the ProtoDUNE-SP detector. A special thanks to Bill Miller and the Ash-River installation group for the excellent job they did during the installation and commissioning and to the CERN Neutrino Platform which provided enormous technician and engineering support.

## References

- [1] DUNE collaboration, B. Abi et al., *The DUNE Far Detector Interim Design Report Volume 1: Physics, Technology and Strategies*, [arXiv:1807.10334](#).
- [2] DUNE collaboration, B. Abi et al., *The DUNE Far Detector Interim Design Report Volume 2: Single Phase Module*, [arXiv:1807.10327](#).
- [3] DUNE collaboration, B. Abi et al., *The DUNE Far Detector Interim Design Report Volume 3: Dual Phase Module*, [arXiv:1807.10340](#).
- [4] DUNE collaboration, B. Abi et al., *The Single-Phase ProtoDUNE Technical Design Report*, [arXiv:1706.07081](#).
- [5] V. Radeka et al., *Cold electronics for 'Giant' Liquid Argon Time Projection Chambers*, *J. Phys. Conf. Ser.* **308** (2011) 012021.
- [6] F. Liu et al., *Cold Electronics System Development for ProtoDUNE-SP and SBND LAr TPC*, *Proceedings of the 2017 IEEE Nuclear Science Symposium and Medical Imaging Conference* (2018) 879–883, [[ISBN 978-1-5386-2283-4](#)].
- [7] H. Chen et al., *Cold Electronics Readout System for ProtoDUNE-SP LAr-TPC*, *Nucl. Instrum. Meth. A* **936** (2019) 271–273.
- [8] G. De Geronimo et al., *Front-end asic for a liquid argon tpc*, *IEEE Transactions on Nuclear Science* **58** (2011) 1376–1385.
- [9] S. Li et al., *LAr TPC Electronics CMOS Lifetime at 300 K and 77 K and Reliability Under Thermal Cycling*, *IEEE Transactions on Nuclear Science* **60.6** (2013) 4737–4743.
- [10] MicroBooNE collaboration, R. Acciarri et al., *Noise Characterization and Filtering in the MicroBooNE Liquid Argon TPC*, *JINST* **12** (2017) P08003, [[arXiv:1705.07341](#)].
- [11] F. Takhti, A. Sodagar and R. Lotfi, *Domino ADC: A Novel Analog-to-Digital Converter Architecture*, *Proceedings of 2010 IEEE International Symposium on Circuits and Systems* (2010) 4057–4061, [[978-1-4244-5308-5](#)].
- [12] “femb python git Repository.” [https://github.com/DUNE/femb\\_python](https://github.com/DUNE/femb_python).
- [13] “The JSON Data Interchange Syntax.” <http://www.ecma-international.org/publications/files/ECMA-ST/ECMA-404.pdf>.
- [14] “femb doc git Repository.” [https://github.com/DUNE/femb\\_doc](https://github.com/DUNE/femb_doc).
- [15] “Sumatra Project.” <https://pypi.org/project/Sumatra/>.